

INVERSE PROBLEM: AN EXPLORATION OF HEAT FLOW

MICHAEL MCKENZIE

WHITMAN COLLEGE 2008-2009

ABSTRACT. We discuss the notion of an inverse problem and then explore a particular inverse problem based on the heat equation. A relationship is established between the deformation location within a one-dimensional rod and the heat flux from the ends of the rod. A finite difference method serves as the tool to solve the one-dimensional heat equation that results from a moving heat source and deformation. We show that for certain simple deformations, it is possible to determine the location within the rod using only heat flux measurements at one end.

1. INTRODUCTION

1.1. Inverse Problems. Inverse problems arise in mathematics when the investigator attempts to reverse the traditional approach to a problem. They are often ill-posed, unstable and generally difficult. For example, given an $n \times n$ matrix, a traditional problem is to determine the n eigenvalues. Given n eigenvalues, an inverse problem is to determine the $n \times n$ matrix from which they originated. The inverse problem is ill-posed because there is no unique solution.

The exploration and application of inverse problems are important in Non-Destructive Evaluation (NDE). NDE is a philosophy of engineering that motivates engineers and designers to probe structures such as bridges and buildings for structural flaws without physically damaging or deconstructing the object. With the aid of computers, entire buildings, roadways, and bridges are analyzed as a whole. Thus, the computers test the structures by simulating various conditions in order to examine how the structure will react. For example, a direct problem, knowing the composition of a bridge, is finding the modes of vibration of the bridge. Utilizing the measured modes of vibration of the bridge, the inverse problem is to determine the structural composition and to analyze the structural integrity in the hopes of locating a flaw that may exist. Our paper explores the same concept through heat conductivity.

1.2. Paper Summary. In this paper, we consider the heat equation as it applies to a one-dimensional rod. Given the heat source and the composition of the rod, the direct problem of finding the fluxes at the ends is well understood. We consider the inverse problem of determining the composition knowing the flux and heat source. However, before we do this, we present a few examples to further explore the idea of direct and inverse problems. After examining and solving a few inverse problems related to ordinary differential equations, we move onto the one-dimensional rod utilizing a finite difference method.

2. DIFFERENTIAL INVERSE PROBLEMS

2.1. Hooke's Law and Newton's Law of Motion. We consider a problem related to a spring-mass system as described in Groetsch[1]. Our aim is to solve for an analytic solution of a spring-mass system given a physical description. We begin with Hooke's Law,

$$F = ma = -kx,$$

where F , m , a , k , and x represent the force, mass, acceleration, spring constant, and displacement, respectively. The spring constant k denotes the stiffness of the spring. Hooke's Law is incorporated into Newton's Law of Motion as an external force acting on the mass. Newton's Law of Harmonic Motion is written as

$$(1) \quad m\ddot{y} = -c\dot{y} - ky,$$

where m , c , k , and y represent the mass, damping coefficient, spring constant, and vertical displacement, respectively.

In order to solve Equation (1) for the vertical displacement with respect to time, we try a solution of the form

$$y = e^{rt}$$

for some undetermined parameter r . Now we take the first and second derivatives with respect to t to get

$$\dot{y} = re^{rt}$$

and

$$\ddot{y} = r^2e^{rt}.$$

From here we substitute them back into Equation (1), divide by e^{rt} and collect all terms to get

$$(2) \quad mr^2 + cr + k = 0.$$

Equation (2) is known as the characteristic equation. Three types of motion result from the characteristic equation. In order to explore the three types of motion, we first solve for r using the quadratic formula to get

$$(3) \quad r = \frac{-c \pm \sqrt{c^2 - 4mk}}{2m}.$$

Over-damped, *critically damped*, and *under-damped* are the types of motion that result from Equation (3) depending on the sign of $c^2 - 4mk$ either positive, negative or neither. If $c^2 > 4mk$, then we have a positive number under the square root of the quadratic equation resulting in two real roots dictating the motion of an over-damped system. If $c^2 = 4mk$, then $\sqrt{c^2 - 4mk} = 0$ leaving $-c/2m$ as the real root dictating the motion of a critically damped system. Finally, if $c^2 < 4mk$, then we have two complex roots dictating the motion of an under-damped system.

First, with $c > 2\sqrt{mk}$ and the two real roots, r_1 and r_2 , the corresponding over-damped equation of motion is

$$(4) \quad y = C_1e^{r_1t} + C_2e^{r_2t}$$

where C_1 and C_2 are some arbitrary constants.

Second, with $c = 2\sqrt{mk}$ and the one real root, r , the corresponding critically damped equation of motion is

$$(5) \quad y = e^{rt}(C_1 + C_2t)$$

where again C_1 and C_2 are some arbitrary constants.

Third, with $c < 2\sqrt{mk}$ and the two complex roots, $r = \lambda \pm \mu i$, the corresponding under-damped equation of motion is

$$(6) \quad y = e^{\lambda t}(C_1 \cos(\mu t) + C_2 \sin(\mu t))$$

where $\lambda = \frac{-c}{2m}$ and $\mu = \frac{\sqrt{4mk-c^2}}{2m}$, and where C_1 and C_2 are some arbitrary constants.

In the most general cases an under-damped system oscillates many times before returning to equilibrium due to the sine and cosine terms within the equation, a critically damped system passes through the equilibrium once before returning to the equilibrium without any further oscillations, and an over-damped system returns, without passing through, to equilibrium.

Here we present a useful exercise in NDE. For the sake of safety, it is beneficial to know parameters of the damped spring-mass system of an automobile's suspension. We present two methods of determining these constants from simple measurements of the system. First we can compress the car's suspension and make note of the displacement. Then we keep track of the number of cycles it takes for the amplitude of the oscillations to decrease to a desired percentage, say 10%. Second, we can count the number of cycles within a given time period.

Using a Ruler: Consider an under-damped system, represented by Equation (6), where we know a mass, $m = 1$ kilogram(kg), stretches the spring $x = 0.21$ meters(m). We know that the amplitude decreases 90% after 25 cycles. Our goal is to determine the damping coefficient, c , and the spring constant, k .

In order to find the spring constant, we utilize Hooke's Law, $F = ma = -kx$. We set up the spring and mass vertically such that the mass hangs from the spring. We set $a = g$, the gravitational constant, allowing us to solve for k because there are four variables with three known. Doing so, we find

$$ma = mg = -kx$$

$$k = \frac{-mg}{x} = \frac{-(1)(-9.8)}{0.21} = \frac{140}{3}$$

where the units of the spring constant are N/m (Newton/meter).

Now it is possible to solve for the damping coefficient. In order to solve for c we must understand the physical description. We consider the sine function because it oscillates with a known period of 2π units, where one cycle or oscillation represents one period, which is written as $at = 2\pi$ when $a = 1$. Thus, the 25 cycles last 50π units. For our problem $a = \frac{\sqrt{4mk-c^2}}{2m}$, which means we get

$$(7) \quad \frac{\sqrt{4mk-c^2}}{2m}t = 50\pi.$$

Also, we know that when the mass crosses the equilibrium for the 25th time, the amplitude is 10% of the original size, which is written as

$$(8) \quad 0.1 = e^{\frac{-ct}{2m}}.$$

We solve Equations (7) and (8) for t and equate to get

$$\frac{-2m}{c} \ln(.1) = \frac{100m\pi}{\sqrt{4mk-c^2}}.$$

Since c is the only unknown, we solve to get

$$c = \sqrt{\frac{\ln(.1)^2 4mk}{50^2 \pi^2 + \ln(.1)^2}} \approx 0.21.$$

In Figure 1 we graph our solution, given by Equation (9),

$$(9) \quad y(t) = e^{\frac{-0.21t}{2}} [C_1 \cos(6.8305t) + C_2 \sin(6.8305t)],$$

to compare our solution to the physical description. Since we are only interested in the oscillation amplitude and oscillation frequency, we choose $C_1 = C_2 = 1$ arbitrarily in order to graph.

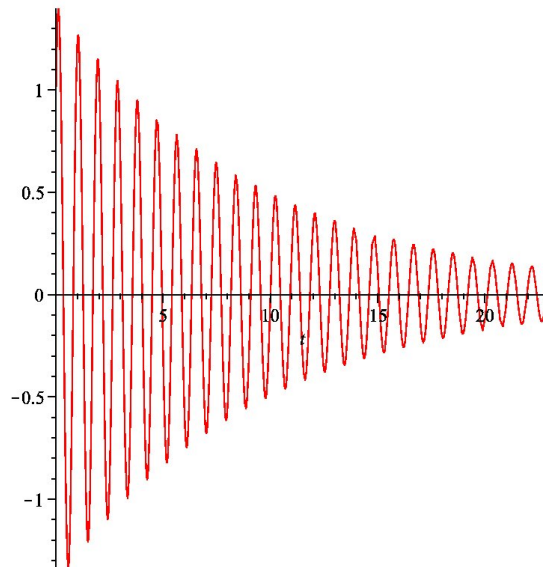


FIGURE 1. With $c \approx 0.21$ and $k = 140/3$, the amplitude of the under-damped system decreases by 90% after 25 cycles.

Using the scale on the vertical axis, we see that once the motion achieves 25 cycles, the amplitude is one-tenth of the original. Thus, our investigation supports the physical description given by Groetsch[1]. The damping coefficient directly influences the rate of decay because it is located in the exponential term of Equation (9). Thus, the amplitude decreases more quickly as c increases. In relation to a vehicle's suspension, we desire a large value of c such that a car does not oscillate when a bump is encountered.

Using a Stopwatch: Consider a critically damped system represented by Equation (5) with $m = 1$ kg, where we know a mass crosses the equilibrium at time $t_1 > 0$ and it reverses its direction at time $t_2 > t_1$. We denote $y(t_1) = 0$ as the time when the mass crosses the equilibrium. Similarly, we denote $\dot{y}(t_2) = 0$ as the time when the mass reverses its direction. We apply $y(t_1) = 0$ to Equation (5) to get

$$(10) \quad y(t_1) = (C_1 + C_2 t_1) e^{\frac{-c t_1}{2m}} = 0,$$

then differentiate Equation (5) with respect to t , and apply $\dot{y}(t_2) = 0$ to get

$$(11) \quad \dot{y}(t_2) = e^{\frac{-ct_2}{2m}} \left[C_1 \left(\frac{-c}{2m} \right) + C_2 \left(1 - \frac{ct_2}{2m} \right) \right] = 0.$$

Now divide Equation (10) and Equation (11) by $e^{-ct_1/2m}$ and $e^{-ct_2/2m}$, respectively, to get

$$C_1 + C_2 t_1 = 0$$

and

$$C_1 \left(\frac{-c}{2m} \right) + C_2 \left(1 - \frac{ct_2}{2m} \right) = 0.$$

Note that we have two equations with three unknowns. Solve Equation (10) for C_1 and substitute into Equation (11), along with $m = 1$, to get

$$-C_2 t_1 \left(\frac{-c}{2} \right) + C_2 \left(1 - \frac{ct_2}{2} \right) = 0.$$

In order to explore the nontrivial case, we assume that $C_2 \neq 0$, such that after some light algebraic manipulation, C_2 disappears leaving

$$1 - \frac{c}{2} t_2 = \frac{-c}{2} t_1.$$

Now we solve for c to get

$$c = \frac{2}{t_2 - t_1}.$$

Recall that we have a critically damped system where $c = 2\sqrt{mk}$. With $m = 1$ and with c known, we solve for k to get

$$k = \frac{1}{(t_2 - t_1)^2}.$$

Thus, in a critically damped system, given the time a mass, $m = 1$, crosses the equilibrium, and the time the mass reverses its direction, directly following the crossing, the time difference $t_2 - t_1$ allows us to directly calculate the damping coefficient, c , and the stiffness coefficient k . More generally

$$c = \frac{2m}{t_2 - t_1}$$

and

$$k = \frac{m}{(t_2 - t_1)^2}$$

where m is any mass. Thus, for a large mass such a car, a large value for the damping coefficient and spring constant is necessary to minimize the oscillations making for a smooth ride.

2.2. Examples Conclusion. The ruler example is an inverse problem because we know the mass and displacement, allowing us to find the spring constant and damping coefficient based only on the number of cycles and the change in amplitude. The time example is an inverse problem because we know the mass and a time the mass crosses the equilibrium along with the time immediately following when it mass reverses its direction allowing us to find the damping coefficient and the spring constant. Using simple tools like a ruler or stopwatch, we can evaluate the integrity of a car's suspension effectively without any deconstruction.

3. AN INVERSE HEAT CONDUCTION PROBLEM

3.1. Introduction of the Heat Equation. We have seen a couple of simple inverse problems. Now we present the one-dimensional heat equation for a one-dimensional rod defined as

$$c\rho\frac{\partial u}{\partial t} = \frac{\partial}{\partial x}\left(K_0\frac{\partial u}{\partial x}\right) + Q$$

where c is the specific heat of the rod, ρ is the mass density of the rod, K_0 is the heat conductivity of the rod, Q is the heat source, and $u(x, t)$ is the temperature of the rod at a given time t and a given position x as given in Haberman[2]. We assume for our exploration that K_0 , c , and ρ are greater than zero and piecewise constant for each section of the rod, and Q is piecewise constant. We reduce the number of constants by dividing the heat equation by $c\rho$ throughout and defining a new constant

$$k = \frac{K_0}{c\rho}$$

which we call the thermal diffusivity of the rod. The thermal diffusivity describes how quickly the heat will spread, or diffuse, throughout the rod. For example, if the heat conductivity of the rod, K_0 , increases, then k increases and it is easier for heat to travel throughout the rod, allowing heat to diffuse more quickly. If c , the specific heat, increases, then k decreases and the rate of diffusion decreases because more heat energy is required to increase the temperature within the rod. Similarly, if the mass density increases, then the thermal diffusivity decreases.

The inverse problem we would like to consider is determining the correlation between thermal diffusivity and heat flux. We model the inverse problem using a “triple-rod” construction. A triple-rod is, in essence, three separate rods that are joined together in perfect thermal contact (PTC)[2], described in more detail below, where the two rods on the outside are made of the same material with the same thermal diffusivity, and the rod in the middle is an unknown material with an unknown thermal diffusivity. We assume that the rod in the middle is much smaller and is intended to represent some kind of damage in an otherwise uniform rod. From analyzing the triple-rod, we seek to establish a relationship between the location of a deformation and the heat flux from the ends of the rod. Fourier’s Law of Heat Flux is given by

$$(12) \quad \Phi = -ku'$$

where Φ is the heat flux, k is the thermal diffusivity, and u' is the change in temperature. Fourier’s Law is crucial at the locations where the two outer rods contact the inner rod of the triple-rod system in an end-to-end fashion. At the point of PTC, the rate at which heat flows from one material into the other is directly proportional to the thermal diffusivity of the rod it is leaving and the rod it is entering. So, with a given source in a particular location, we seek to identify the location of the middle rod based upon the rate at which heat flows from the ends of the entire triple-rod system.

In order to clarify the nature of this inverse problem, imagine we have a track that is 100 meters in length and two identical runners, named Jack and Jerry, line up back to back at the middle of the track so each has 50 meters to run. Both runners will run at the exact same speed, however, 25 meters from Jerry, there is a path 15 meters in length that is nothing but sand. Both runners take off at the

exact same time running in opposite directions. A bystander in the grandstands watches the entire race take place. She notices that for the first 25 meters they are equal, but as soon as each runner passes this distance, Jerry, slows down due to the sand. By the time Jerry makes it through the sand, Jack gains a lead and finishes first. Based upon a change in Jerry's path, his progress was slowed. If we make one more assumption in that there was yet another observer who knew about the previous conditions except for the sand and could not see the track except for the ends, then her observations would lead her to believe that something had prevented Jerry from reaching the end at the same moment as Jack.

Our approach to the triple-rod problem is that of the observer who could only see the ends of the track. We solve the direct problem in order to establish a relationship between a deformation and heat flux from the ends of the triple-rod. The inverse problem is using experimental data of heat fluxes in order to locate the deformation. In order to do so, we must have knowledge of the composition of the original undamaged rod. An ideal solution would provide enough detail in order to identify the composition of the deformed material.



FIGURE 2. PTC occurs at $x = \alpha$. The section of the rod from $0 < x < \alpha$ is represented by ϕ_1 , and the section of the rod from $\alpha < x < L$ is represented by ϕ_2 .

3.2. Dual-Rod Without Sources. Before we consider the full triple-rod construction we consider a one-dimensional rod composed of two different materials in PTC at $x = \alpha$. PTC means that the heat flow, or flux, out of one part of the rod at α equals the heat flow into the other, and the the temperatures in the two materials at this location are equal. We denote the PTC conditions by

$$u(\alpha^-, t) = u(\alpha^+, t)$$

and

$$k_1 u_x(\alpha^-, t) = k_2 u_x(\alpha^+, t)$$

where $u(\alpha^-, t)$ is the temperature on the left side of α , $u(\alpha^+, t)$ is the temperature on the right side of α , $k_1 u_x(\alpha^-, t)$ is the heat flux to the left of α , $k_2 u_x(\alpha^+, t)$ is the heat flux to the right of α , k_1 is the thermal diffusivity for the left end of the rod, and k_2 is the thermal diffusivity for the right end of the rod. Also, we assume the rod is insulated such that any heat flow out of the system occurs solely at the ends of the rod. The temperatures at the ends are $u(0, t) = 0$ and $u(L, t) = 0$ for $t > 0$. For $0 < x < \alpha$, we set $k_1 = 1$, and for $\alpha < x < L$, we set $k_2 = 2$. It is important to note that the boundary conditions for our problem are unnatural. Since the temperature is held at zero at each end, and heat is exiting the rod, it takes work to keep the temperature held at zero. For both materials, there are no sources, $Q = 0$.

The Heat Equation is defined by

$$(13) \quad c\rho \frac{\partial u}{\partial t} = \frac{\partial}{\partial t} \left(K_0 \frac{\partial u}{\partial t} \right) + Q.$$

Since we have no sources and are concerned with the conductivity, k , we rewrite Equation (13) as

$$(14) \quad \frac{\partial u}{\partial t} = \frac{\partial}{\partial x} \left(k \frac{\partial u}{\partial x} \right)$$

where $k = \frac{K_0}{c\rho}$. We now introduce the separation of variables $u(x, t) = \phi(x)h(t)$, which yields

$$(15) \quad h' \phi = h \frac{\partial}{\partial x} \left(k \frac{\partial \phi}{\partial x} \right) = h(k\phi)'$$

where $h(t)$ represents the time component and $\phi(x)$ represents the space component.

We proceed considering the space component. We introduce a constant λ that is real because we are analyzing a self-adjoint eigenvalue problem. Our boundary conditions ensure that $\lambda \geq 0$. However, we further restrict $\lambda > 0$ because we are using prescribed boundary conditions. Thus after separation of variables the space equation is

$$(16) \quad (k\phi)' + \lambda\phi = 0.$$

However, k is piecewise constant so we rewrite Equation (16) as

$$(17) \quad k\phi'' + \lambda\phi = 0.$$

For our dual-rod, we generalize Equation (17) into

$$(18) \quad k_1\phi_1'' + \lambda\phi_1 = 0, \quad 0 < x < \alpha$$

$$(19) \quad k_2\phi_2'' + \lambda\phi_2 = 0, \quad \alpha < x < L$$

where $k_1 = 1$ and $k_2 = 2$. Thus Equation (18) gives the equation

$$(20) \quad \phi_1(x) = c_1 \cos(\sqrt{\lambda}x) + c_2 \sin(\sqrt{\lambda}x).$$

We apply the boundary condition $u(0, t) = 0$ to Equation (20) finding $c_1 = 0$. Thus, Equation (20) is simplified to

$$(21) \quad \phi_1(x) = c_2 \sin(\sqrt{\lambda}x).$$

Similarly, Equation (19) is equivalent to

$$\phi_2'' + \frac{\lambda}{2}\phi_2 = 0,$$

and gives the equation

$$(22) \quad \phi_2(x) = d_1 \cos\left(\sqrt{\frac{\lambda}{2}}x\right) + d_2 \sin\left(\sqrt{\frac{\lambda}{2}}x\right).$$

We apply the boundary condition $u(L, t) = 0$ to Equation (22) finding

$$d_1 = -\tan\left(\sqrt{\frac{\lambda}{2}}L\right)d_2.$$

Thus Equation 22 is simplified to

$$(23) \quad \phi_2(x) = d_2 \left[\sin\left(\sqrt{\frac{\lambda}{2}}x\right) - \tan\left(\sqrt{\frac{\lambda}{2}}L\right) \cos\left(\sqrt{\frac{\lambda}{2}}x\right) \right].$$

We apply the first PTC condition $\phi_1(\alpha) = u(\alpha^-, t) = u(\alpha^+, t) = \phi_2(\alpha)$, and then differentiate Equation (21) and Equation (23) with respect to x in order to apply the second PTC condition $\phi_1'(\alpha) = k_1 u_x(\alpha^-, t) = k_2 u_x(\alpha^+, t) = 2\phi_2'(\alpha)$. These two boundary conditions provide the two equations

$$c_2 \sin(\sqrt{\lambda}\alpha) = d_2 \left[\sin\left(\sqrt{\frac{\lambda}{2}}\alpha\right) - \tan\left(\sqrt{\frac{\lambda}{2}}L\right) \cos\left(\sqrt{\frac{\lambda}{2}}\alpha\right) \right]$$

and

$$c_2 \sqrt{\lambda} \cos(\sqrt{\lambda}\alpha) = d_2 2 \left[\sqrt{\frac{\lambda}{2}} \cos\left(\sqrt{\frac{\lambda}{2}}\alpha\right) + \sqrt{\frac{\lambda}{2}} \tan\left(\sqrt{\frac{\lambda}{2}}L\right) \sin\left(\sqrt{\frac{\lambda}{2}}\alpha\right) \right].$$

We shift all constants to one side of both equations in order to rewrite the system of equations in the following matrix form:

$$A \begin{bmatrix} c_2 \\ d_2 \end{bmatrix} = \begin{bmatrix} 0 \\ 0 \end{bmatrix}$$

where

$$A = \begin{bmatrix} \sin(\sqrt{\lambda}\alpha) & -\sin\left(\sqrt{\frac{\lambda}{2}}\alpha\right) + \tan\left(\sqrt{\frac{\lambda}{2}}L\right) \cos\left(\sqrt{\frac{\lambda}{2}}\alpha\right) \\ \sqrt{\lambda} \cos(\sqrt{\lambda}\alpha) & -2 \left[\sqrt{\frac{\lambda}{2}} \cos\left(\sqrt{\frac{\lambda}{2}}\alpha\right) + \sqrt{\frac{\lambda}{2}} \tan\left(\sqrt{\frac{\lambda}{2}}L\right) \sin\left(\sqrt{\frac{\lambda}{2}}\alpha\right) \right] \end{bmatrix}.$$

Non-trivial solutions to this homogeneous equation exist only if the determinant is zero. The λ 's that cause the determinant to be zero are the eigenvalues of this dual-rod system. We utilize Maple to solve $\det(A) = 0$ in terms of λ and plot the solution curves implicitly.

Figure 3 offers a unique perspective into the inverse problem of the dual-rod. The vertical axis represents the location of α , the point of PTC, while the horizontal axis represents the corresponding first few eigenvalues. Suppose we wish to use the eigenvalues of the system to determine the location of α . If we observe the curve representing the first eigenvalue λ_1 , we see that any slight error in measuring this eigenvalue leads to a large miscalculation in determining the location of α because the line is close to vertical. However, as we move farther out to higher eigenvalues the lines begin to have more shape which means that even with a slight error, we can find the location of α with more precision. There is a trade off though. Consider the vertical line at $\lambda = 400$. This line shows that there exist two eigenvalues that correspond to the same numerical value. As we can see, when $\lambda_5 = 400$ it corresponds to the location of α_2 , and when $\lambda_6 = 400$ it corresponds to the location of α_1 . This is a major concern because α_1 and α_2 reside on opposing sides of the rod. In order to find the most suitable λ , we must find an eigenvalue that allows for some error in measurement, but does not overlap with other eigenvalues. Based upon Figure 3, λ_2 serves as the best choice because λ_3 and λ_4 overlap, and λ_1 is more vertical. This illustrates some of the difficulties that occur in inverse problems.

For additional insight, we check what happens for values of α that essentially reduce the dual-rod to a single uniform rod. First we let $\alpha = 0$ which corresponds to a uniform rod with thermal diffusivity k_2 . Hence, we are interested in the values where

$$d_2 \tan\left(\sqrt{\frac{\lambda}{2}}L\right) = 0.$$

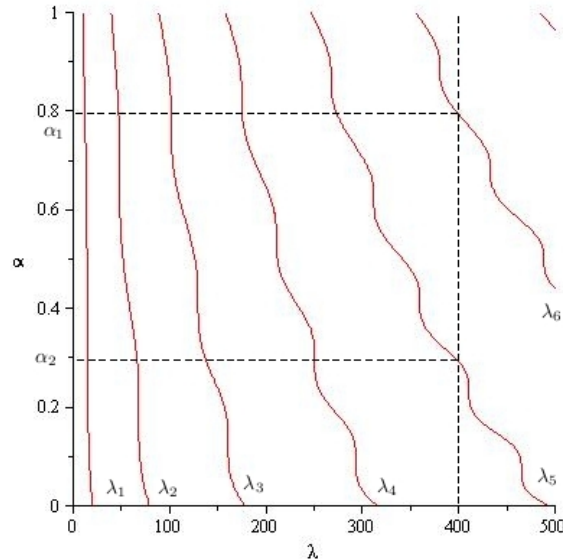


FIGURE 3. With the length of the rod $L = 1$, we have a plot of the eigenvalues, λ , along the horizontal axis and the PTC location α on the vertical axis. The vertical line at $\lambda = 400$ shows how two different eigenvalues can correspond to different locations of PTC. If $\lambda_5 = 400$, we get $\alpha_2 \approx 0.3$. If $\lambda_6 = 400$, we get $\alpha_1 \approx 0.8$.

For a non-trivial solution we examine $\tan(\sqrt{\lambda/2}L) = 0$. Based upon a graph of tangent, we know

$$\sqrt{\frac{\lambda}{2}}L = n\pi \text{ for } n = 1, 2, 3, \dots$$

Hence

$$(24) \quad \lambda_2 = 2\left(\frac{n\pi}{L}\right)^2 \text{ for } n = 1, 2, 3, \dots$$

where these values correspond to the eigenvalues for a uniform rod with thermal diffusivity k_2 .

Now we let $\alpha = L$ which corresponds to a uniform rod with thermal diffusivity k_1 . We are interested in the values where

$$c_2 \sin(\sqrt{\lambda}L) = 0.$$

For a non-trivial solution we examine $\sin(\sqrt{\lambda}L) = 0$. We know that $\sin(\sqrt{\lambda}L) = 0$ when $\sqrt{\lambda}L = n\pi$. Thus,

$$(25) \quad \lambda_1 = \left(\frac{n\pi}{L}\right)^2 \text{ for } n = 1, 2, 3, \dots$$

where these values correspond to the eigenvalues for a uniform rod with thermal diffusivity k_1 .

In Figure 3 we set $L = 1$. The eigenvalues at $\alpha = 0$ and $\alpha = L$ are given by Equations (24) and (25), respectively. Thus, as α moves from 0 to L , the eigenvalues shift from λ_2 to λ_1 .

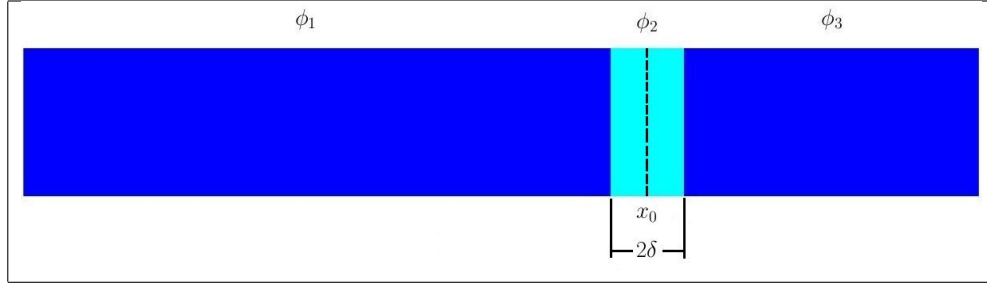


FIGURE 4. PTC occurs at $x = x_0 - \delta$ and $x = x_0 + \delta$. The sections from $0 < x < x_0 - \delta$, $x_0 - \delta < x < x_0 + \delta$, and $x_0 + \delta < x < 1$ are represented by ϕ_1 , ϕ_2 , and ϕ_3 , respectively.

3.3. Triple-Rod with Constant Source. By way of demonstrating some of the techniques we will use on the heat flux inverse problem, we now consider a triple-rod system, but only its long-term behavior. We consider a one dimensional rod composed of two different materials, where one material makes up the two outer portions, while the second material makes up the middle portion. We denote the three portions as

$$\begin{aligned} 0 < x < x_0 - \delta, \\ x_0 - \delta < x < x_0 + \delta \end{aligned}$$

and

$$x_0 + \delta < x < L,$$

where x_0 is the center of the “deformation” and δ represents the distance from x_0 to the other material. For regions one and three, $k = k_0$, and for region two, the middle region, $k = k_0 + \epsilon$, where k again represents the thermal diffusivity of the rod and ϵ represents a shift in the thermal diffusivity. Also, there is a constant heat source Q throughout the rod. Finally, we are interested in the long-term solution of the heat equation, where the heat traveling throughout the rod does not change with time, thus $\partial u / \partial t = 0$.

Similar to the dual-rod, we have boundary conditions for the ends of the rods as well as internal conditions for the locations where the different rods are in PTC. Hence we now have six conditions to consider, where

$$(26) \quad \begin{aligned} u(0) &= 0 \\ u(L) &= 0 \end{aligned}$$

are the boundary conditions,

$$(27) \quad \begin{aligned} u(x_0 - \delta^-) &= u(x_0 - \delta^+) \\ k_0 u'(x_0 - \delta^-) &= (k_0 + \epsilon) u'(x_0 - \delta^+) \end{aligned}$$

are the PTC conditions at $x_0 - \delta$, and

$$(28) \quad \begin{aligned} u(x_0 + \delta^-) &= u(x_0 + \delta^+) \\ (k_0 + \epsilon) u'(x_0 + \delta^-) &= k_0 u'(x_0 + \delta^+) \end{aligned}$$

are the PTC conditions at $x_0 + \delta$. The long-term equation is given by

$$0 = k\phi'' + Q$$

because k is piecewise constant in each region and $\partial u/\partial t = 0$. The general solution is given by

$$(29) \quad \phi(x) = \frac{-Q}{2k}x^2 + a_1x + a_2$$

where a_1 and a_2 are constants.

For $0 < x < x_0 - \delta$, our equation is

$$(30) \quad \phi_1(x) = \frac{-Q}{2k_0}x^2 + c_1x + c_2$$

where c_1 and c_2 are constants. For the region $0 < x < x_0 - \delta$, we apply the boundary condition $u(0) = 0$ to Equation (30) to find $c_2 = 0$ which allows us to rewrite the equation as

$$\phi_1(x) = \frac{-Q}{2k_0}x^2 + c_1x.$$

For $x_0 + \delta < x < L$, our equation is

$$(31) \quad \phi_3(x) = \frac{-Q}{2k_0}x^2 + b_1x + b_2.$$

We apply the boundary condition $u(L) = 0$ finding $b_2 = \frac{Q}{2k_0}L^2 + b_1L$. Thus, for the region $x_0 + \delta < x < L$, our equation is

$$\phi_3(x) = \frac{Q}{2k_0}(L^2 - x^2) + b_1(x + L).$$

For $x_0 - \delta < x < x_0 + \delta$, our equation is

$$(32) \quad \phi_2(x) = \frac{-Q}{2(k_0 + \epsilon)}x^2 + d_1x + d_2.$$

After applying the PTC conditions, we get four linear equations

$$\frac{-Q}{2k_0}(x_0 - \delta)^2 + c_1(x_0 - \delta) = \frac{-Q}{2(k_0 + \epsilon)}(x_0 + \epsilon)^2 + d_1(x_0 - \delta) + d_2,$$

$$-Q(x_0 - \delta) + c_1k_0 = -Q(x_0 - \delta) + d_1(k_0 + \epsilon),$$

$$\frac{-Q}{2(k_0 + \epsilon)}(x_0 + \epsilon)^2 + d_1(x_0 + \delta) + d_2 = \frac{Q}{2k_0}(L^2 - (x_0 + \delta)^2) + b_1((x_0 + \delta) + L),$$

and

$$-Q(x_0 + \delta) + d_1(k_0 + \epsilon) = \frac{Q}{2}(L^2 - 2(x_0 + \delta)) + b_1k_0.$$

The next big challenge involves solving this system of four linear equations for the four unknowns c_1 , d_1 , d_2 , and b_1 . Using Maple, we find

$$c_1 = \frac{1}{2} \frac{Q(-4x_0\delta\epsilon + L^2k_0 + L^2\epsilon)}{k_0(Lk_0 - 2\delta\epsilon + L\epsilon)},$$

$$d_1 = \frac{1}{2} \frac{Q(-4x_0\delta\epsilon + L^2k_0 + L^2\epsilon)}{-2k_0\delta\epsilon - 2\delta\epsilon^2 + 2Lk_0\epsilon + L\epsilon^2 + Lk_0^2},$$

$$d_2 = \frac{1}{2} \frac{1}{k_0(k_0 + \epsilon)(Lk_0 - 2\delta\epsilon + L\epsilon)} Q\epsilon(k_0x_0L^2 + 2k_0x_0\delta L - k_0x_0^2L - k_0\delta L^2 - k_0\delta^2L - \delta^2L\epsilon + 2x_0\delta L\epsilon + x_0L^2\epsilon - x_0^2L\epsilon - \delta L^2\epsilon + 2\delta^3\epsilon - 2x_0^2\delta\epsilon),$$

and

$$b_1 = \frac{1}{2} \frac{Q(-4x_0\delta\epsilon + L^2k_0 + L^2\epsilon)}{k_0(Lk_0 - 2\delta\epsilon + L\epsilon)}.$$

We substitute c_1 and b_1 back into ϕ'_1 and ϕ'_3 respectively to get

$$\phi'_1(0) = \frac{1}{2} \frac{Q(-4x_0\delta\epsilon + L^2k_0 + L^2\epsilon)}{k_0(Lk_0 - 2\delta\epsilon + L\epsilon)}$$

and

$$\phi'_3(L) = -\frac{QL}{k_0} + \frac{Q(-4x_0\delta\epsilon + L^2k_0 + L^2\epsilon)}{k_0(Lk_0 - 2\delta\epsilon + L\epsilon)}.$$

We note that the second term in $\phi'_3(L)$ is $2\phi'_1(0)$. Hence we have the following relationship

$$(33) \quad \phi'_3(L) = \frac{-QL}{k_0} + 2\phi'_1(0),$$

which gives a relationship between the fluxes at both ends, but does not provide any information about the deformation.

Equation (33) shows that measuring the fluxes at both ends of the rod does not provide any data regarding the location of the deformation within the rod. The constant heat source over the entire rod does not allow for the location of the deformation to be found because the diffusivity of the two outer rods compensates for the deformation. This means that the heat travels through the non-deformation material at the same rate. Thus, the introduction of the uniform heat source does not provide any insight into the location or size of the deformation.

3.4. Triple-Rod with Moving Source. As can be seen in Figure 5, the triple-rod with a moving source has the exact same set up with respect to the regions, boundary conditions, and long term equation as the previous triple-rod with a constant source. The difference here is that the source term Q is piecewise constant and is designed to model an inspector moving the heat source along the exterior length of the rod. We introduce the source term at specific intervals. A moving source combined with the triple-rod model produces five cases to consider. In each case \bar{x}_1 and \bar{x}_2 represent the left and right ends of the moving source respectively. Also, we now denote the deformation location by \bar{x}_0 .

Case	Location of Source
<i>I</i>	$0 < \bar{x}_1 < \bar{x}_2 < \bar{x}_0 - \delta$
<i>II</i>	$0 < \bar{x}_1 < \bar{x}_0 - \delta < \bar{x}_2$
<i>III</i>	$0 < \bar{x}_1 < \bar{x}_0 - \delta < \bar{x}_0 + \delta < \bar{x}_2 < L$
<i>IV</i>	$\bar{x}_0 - \delta < \bar{x}_1 < \bar{x}_0 + \delta < \bar{x}_2 < L$
<i>V</i>	$\bar{x}_0 + \delta < \bar{x}_1 < \bar{x}_2 < L$

Case one represents a location where the heat source resides entirely in the left most rod. Case two represents a location where the heat source overlaps the left and middle rods. Case three represents a location where the heat source overlaps the three rods. Case four represents a location where the heat source overlaps the middle and right rods. Finally, case five represents a location where the heat source resides entirely in the right most rod. Figure 5 gives pictorial representations of the five cases. Unfortunately, attempting to solve these cases using our methods from the triple-rod with a constant source proves to be an algebraic nightmare. Thus, we

lower our goals, take a numerical approach to solving this system using the finite difference method, and show that the inverse problem has a unique solution.

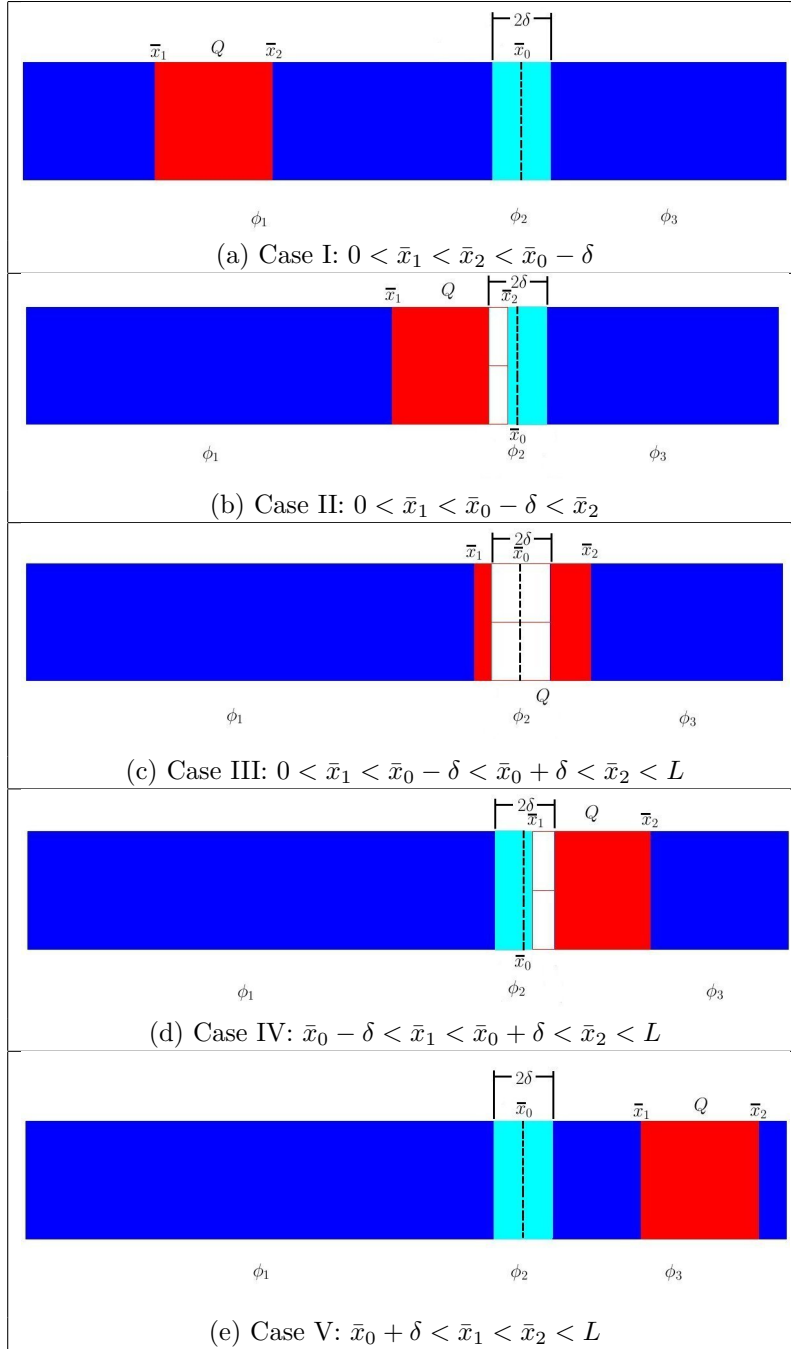


FIGURE 5.

4. AN INVERSE HEAT CONDUCTION PROBLEM

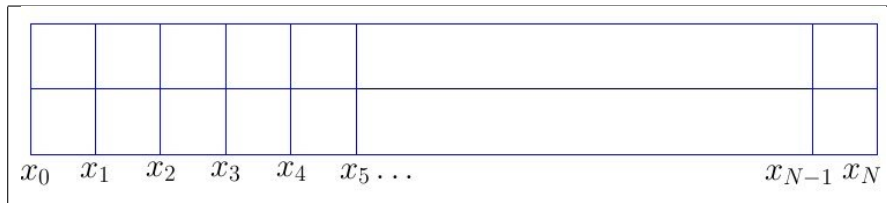


FIGURE 6.

We are now ready to consider the full inverse heat conduction problem. Consider heat flow in a “damaged” metal rod of length one. We control the heat source, Q , and assume that the unknown heat conductivity, k , is piecewise constant. We are allowed to change the location of the heat source and measure the heat flow out of the ends. Using this information we determine the location and magnitude of the damage within the rod. For our analysis, we model the source term, Q , as a piecewise constant function. We are interested in the long-term, time independent, solution of the heat equation where we assume $\partial u/\partial t = 0$. Under these assumptions, the heat equation is

$$(34) \quad \frac{\partial}{\partial x} \left[k(x) \frac{\partial}{\partial x} \phi(x) \right] + Q(x) = 0$$

where $k(x)$ and $Q(x)$ are piecewise constant.

We use a numerical set of solutions to show that this inverse problem is solvable. We discretize our rod into N pieces of equal size, and let h be the distance between each point. That is

$$h = \frac{1}{N}$$

and let

$$x_i = \frac{i}{N} \text{ for } i = 0, 1, \dots, N$$

represent the different points along the rod beginning with $x_0 = 0$ and ending with $x_N = 1$.

Next we set up the finite difference equations to approximate the long-term solutions of the heat equation. Then we plot heat flow versus the damage location to show that it is possible to determine the damage location solely from measuring heat flow.

The finite difference approximation of the first derivative is given by

$$(35) \quad f'(x) = \frac{f(x+h) - f(x-h)}{2h} + O(h)$$

where $h = \frac{1}{N}$ and $O(h)$ is the truncation error.

Now apply this result to Equation (34). We ignore the $Q(x)$ term at this moment in order to concentrate solely on the $\frac{\partial}{\partial x} [k(x) \frac{\partial}{\partial x} \phi(x)]$ term:

$$\begin{aligned} \frac{\partial}{\partial x} [k(x) \frac{\partial}{\partial x} \phi(x)] &\approx \frac{\partial}{\partial x} \left[k(x) \left(\frac{\phi(x+h) - \phi(x-h)}{2h} \right) \right] \\ &\approx \frac{\partial}{\partial x} \left[\frac{k(x+h) - k(x-h)}{2h} \left[\frac{\phi(x+h) - \phi(x-h)}{2h} \right] \right. \\ &\quad \left. + \frac{k(x)}{2h} \left[\left(\frac{\phi(x+2h) - \phi(x)}{2h} \right) - \left(\frac{\phi(x) - \phi(x-2h)}{2h} \right) \right] \right] \\ &\approx \frac{k(x)}{4h^2} \phi(x+2h) + \frac{k(x+h) - k(x-h)}{4h^2} \phi(x+h) - \frac{2k(x)}{4h^2} \phi(x) \\ &\quad + \frac{k(x-h) - k(x+h)}{4h^2} \phi(x-h) + \frac{k(x)}{4h^2} \phi(x-2h) \end{aligned}$$

In order to apply this to our rod, we substitute h and x_i , which gives a system of linear equations whose solution is the approximate long-term solution given by

$$(36) \quad \frac{\partial}{\partial x} [k(x_i) \frac{\partial}{\partial x} \phi(x_i)] + Q(x_i) \approx \frac{k(x_i)}{4/N^2} \phi(x_{i+2}) + \frac{k(x_{i+1}) - k(x_{i-1})}{4/N^2} \phi(x_{i+1}) \\ - \frac{2k(x_i)}{4/N^2} \phi(x_i) + \frac{k(x_{i-1}) - k(x_{i+1})}{4/N^2} \phi(x_{i-1}) \\ + \frac{k(x_i)}{4/N^2} \phi(x_{i-2}) + Q(x_i).$$

We denote Equation (36) as the finite difference heat equation. It is important to note that we consider the first and last rows separately in order to incorporate the boundary conditions. We now approximate the $\phi(x_i)$'s, which are the solutions to the differential equation at x_i . We do not need to evaluate at x_0 or x_N because

$$\phi(x_0) = \phi(0) = 0$$

and

$$\phi(x_N) = \phi(1) = 0.$$

In matrix form, the system of linear equations is given by

$$\Phi = \begin{bmatrix} C_1 & D_2 & E_3 & 0 & & & & & \cdots & 0 \\ B_1 & C_2 & D_3 & E_4 & 0 & & & & \cdots & 0 \\ A_1 & B_2 & C_3 & D_4 & E_5 & 0 & & & \cdots & 0 \\ 0 & A_2 & B_3 & C_4 & D_5 & E_6 & 0 & & \cdots & 0 \\ 0 & 0 & \ddots & \ddots & \ddots & \ddots & \ddots & 0 & \cdots & 0 \\ \vdots & & & & & & & & & \vdots \\ 0 & \cdots & & 0 & \ddots & \ddots & \ddots & \ddots & \ddots & 0 \\ 0 & \cdots & & & 0 & A_{N-5} & B_{N-4} & C_{N-3} & D_{N-2} & E_{N-1} \\ 0 & \cdots & & & & 0 & A_{N-4} & B_{N-3} & C_{N-2} & D_{N-1} \\ 0 & \cdots & & & & & 0 & A_{N-3} & B_{N-2} & C_{N-1} \end{bmatrix}$$

where

$$\begin{aligned} E_{i+2} &= \frac{k(x_i)}{4/N^2} && \text{for } i = 1 \dots N-3 \\ D_{i+1} &= \frac{k(x_{i+1}) - k(x_{i-1})}{4/N^2} && \text{for } i = 1 \dots N-2 \\ C_i &= \frac{-2k(x_i)}{4/N^2} && \text{for } i = 1 \dots N-1 \\ B_{i-1} &= \frac{k(x_{i-1}) - k(x_{i+1})}{4/N^2} && \text{for } i = 2 \dots N-1 \\ A_{i-2} &= \frac{k(x_i)}{4/N^2} && \text{for } i = 3 \dots N-1 \end{aligned}$$

This then allows us to write the system of equations as

$$\Phi \begin{bmatrix} \phi(x_1) \\ \phi(x_2) \\ \vdots \\ \phi(x_{N-1}) \end{bmatrix} = \begin{bmatrix} -Q(x_1) \\ -Q(x_2) \\ \vdots \\ -Q(x_{N-1}) \end{bmatrix} \quad \text{for } i=1,2,\dots,N-1.$$

We now address the top and bottom rows of Φ because our current terms cannot be evaluated. As we approach the ends of the rod, some of these terms become nonsensical because they represent a portion of the rod that does not exist. In the first row A_{i-2} and in the last row E_{i+2} are the terms that cannot be evaluated.

In fact the first and last rows of the matrix Φ must be found using a separate approximation. The first row, the term A_{i-2} cannot be evaluated because it uses points outside the domain of the rod. A similar issue occurs in the last row with E_{i+2} . It is important to recognize that there are two columns that are not included in the matrix Φ . These columns relate to $\phi(x_0)$ and $\phi(x_N)$ which we know to be zero.

Now we handle the issues regarding the first and last rows of Φ . We approximate the first row by

$$\begin{aligned} & (k(x_1)\phi'(x_1))' \\ & \approx \frac{k(x_2)[\phi(x_3) - \phi(x_1)] - k(x_1)\phi(x_2)}{2h^2} \\ & \approx \frac{1}{2h^2} [-k(x_2)\phi(x_1) - k(x_1)\phi(x_2) + k(x_2)\phi(x_3)], \end{aligned}$$

and we approximate the last row by

$$\begin{aligned} & (k(x_{n-1})\phi'(x_{N-1}))' \\ & \approx \frac{1}{2h^2} [k(x_{N-2})\phi(x_{N-3}) - k(x_{N-1})\phi(x_{N-1}) - k(x_{N-2})\phi(x_{N-1})]. \end{aligned}$$

We solve the resulting linear systems with the help of the Lapack++ numerical linear algebra C++ library.

5. GRAPHICAL ANALYSIS

For our graphical analysis, we discretize our rod of length $L = 1$ into 100 pieces. We set the heat source to a length that is one-fifth the length of the rod and a height of $Q = 1$. The locations of the left and right ends of the heat source are denoted by \bar{x}_1 and \bar{x}_2 , respectively. The deformation has a width $\delta = 0.05$ centered about a point \bar{x}_0 . The heat conductivity of the rod is set to $k_0 = 1$. The difference in the height of the heat conductivity between the original rod and the deformation is denoted by ϵ . We vary ϵ from 0 to -0.9 . That is, when $\epsilon = 0$, the triple-rod system behaves as a single uniform rod because

$$k_0 = 1 = k_0 + \epsilon,$$

and when the heat conductivity is -0.9 , the effective heat conductivity in the deformation is

$$k_0 + \epsilon = 1 - 0.9 = 0.1.$$

We note that the left flux is negative due to the orientation of the rod. Since the value of x increases to the right, heat flowing to the left is moving in a negative direction.

We initialize the program with $\bar{x}_0 = 0.05$, $\bar{x}_1 = 0$, and $\bar{x}_2 = 0.2$. We use Lapack++ to solve the system numerically for the left flux. Then we shift the heat source such that $\bar{x}_1 = 0.2$ and $\bar{x}_2 = 0.4$, and we solve for the left flux again. The process of shifting the heat source and solving the system for the left flux is repeated until $\bar{x}_2 = 1$. That is, for each deformation location there are five heat source locations for which we calculate and record the left flux. Once $\bar{x}_2 = 1$, we shift the heat source back to $\bar{x}_1 = 0$ and $\bar{x}_2 = 0.2$, and we shift the deformation such that $\bar{x}_0 = 0.1$. Then we loop through the process again until $\bar{x}_0 + \delta = 1$ and $\bar{x}_2 = 1$. Figure 7 shows a plot of the left flux versus the deformation location \bar{x}_0 with $\epsilon = -0.5$.

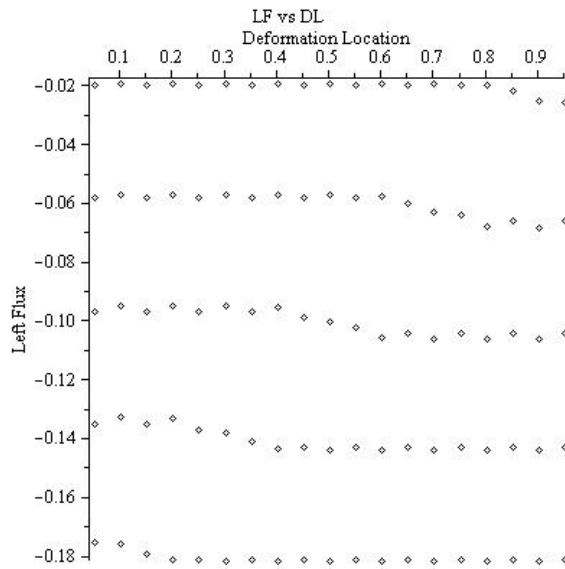


FIGURE 7. Left flux vs. \bar{x}_0 with $\epsilon = -0.5$. The left flux is negative because the heat is moving in the negative direction in relation to the rod.

The five lines of data points in Figure 7 correspond to the five positions of the heat source in the rod. For each heat source position there are 19 data points which correspond to the positions of the deformation.

In Figure 7, consider the bottom row of data points, those that lie on or close to the value -0.18 . This row of data corresponds to the heat source located at $\bar{x}_1 = 0$ and $\bar{x}_2 = 0.2$ because the left heat flux is the most negative. Remember, that the heat is moving in a negative direction. In examining this heat source location we see that when the deformation is located at $\bar{x}_0 = 0.05$, $\bar{x}_0 = 0.1$, and $\bar{x}_0 = 1.5$, the left flux is less negative. This is a direct correlation to the deformation which acts a barrier reducing the rate that heat flows. When $\bar{x}_0 = 0.2$, a majority of the heat source lies to the left of the deformation allowing the heat to flow unrestricted from the left end. We also note that as the deformation moves along the positive x direction within the heat source, the left heat flux becomes more negative.

Now in Figure 7, consider the second row of data from the bottom. This corresponds to the heat source at $\bar{x}_1 = 0.2$ and $\bar{x}_2 = 0.4$ because we used this data and

it is consistent with our expectations. As the heat source moves farther towards the positive x direction of the triple rod system, the left heat flux becomes less negative. Because of this the middle, second from the top, and top rows correspond to the heat source located at $\bar{x}_1 = 0.4$ and $\bar{x}_2 = 0.6$, $\bar{x}_1 = 0.6$ and $\bar{x}_2 = 0.8$, and $\bar{x}_1 = 0.8$ and $\bar{x}_2 = 1.0$ respectively. With each heat source location we find a relationship between the heat source location and the deformation location. However, even when the heat source does not overlap the deformation, it is possible to determine which direction to shift the heat source in order to locate the deformation. Since we calculate the expected left heat flux of a uniform rod, if the measured heat flux is less negative, then the deformation lies to the right of the heat source, and if the measured heat flux is more negative, then the deformation lies to the left of the heat source.

We repeat the aforementioned process for $\epsilon = 0, -0.1, -0.2, \dots, -0.9$. Figure 8 represents all of the data.

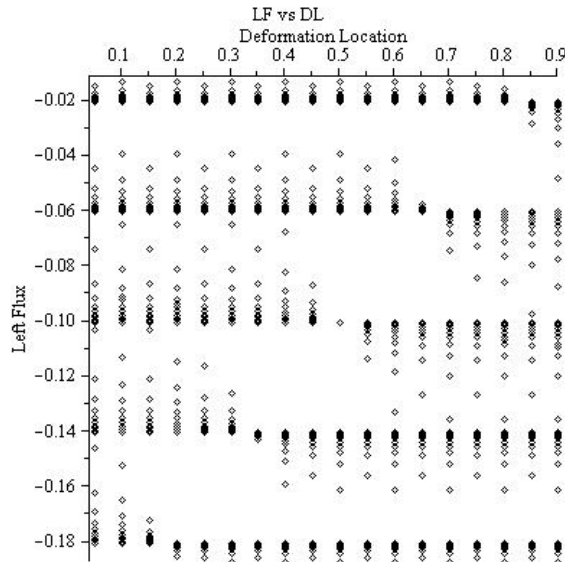


FIGURE 8. Left flux vs. \bar{x}_0 with $\epsilon = 0, -0.1, -0.2, \dots, -0.9$. The left flux is negative because the heat is moving in the negative direction in relation to the rod. The most negative row of flux values correspond to the $\bar{x}_1 = 0$ and $\bar{x}_2 = 0.2$.

From our previous analysis of $\epsilon = -0.5$, we expect to observe a similar pattern of correlation between the left flux and the deformation location. From Figure 8, we see that the pattern does exist with other values of ϵ . In fact, the greater the difference in heat conductivity between the original material and the deformed material, the greater the shift in the left heat flux as the heat source and deformation move. However, as ϵ becomes more negative, the value of the left heat flux fluctuates to a larger degree. These fluctuations are due to the approximation of our finite difference formulas. Thus, with any value of $-1 < \epsilon < 0$, we can locate a deformation within a one-dimensional rod.

6. CONCLUSION

We showed it is possible to locate a deformation within a one-dimensional rod by introducing a heat source at a known location and measuring the heat flux from one end of the rod. Since our inverse problem depended on the spacial dimensions, namely the locations and widths of the deformation and heat source, one might further explore the one-dimensional rod by discretizing the rod into a larger number of segments, as well as adjusting the widths and heights of the heat source and deformation. Investigating the sensitivity of the measurements, such as width and height, would help determine how small of a deformation may be found. Due to the one-to-one correlation between flux and deformation location, one might attempt to find an analytic solution. Furthermore, one might try to repeat this exploration in two and three space dimensions.

REFERENCES

- [1] Groetsch, Charles W. Inverse Problems: Activities for Undergraduates. N.p.: The Mathematical Association of America, 1999.
- [2] Haberman, Richard. Applied Partial Differential Equations with Fourier Series and Boundary Value Problems. New Jersey: Pearson Education, Inc., 2004
- [3] Sauer, Timothy. Numerical Analysis. Boston: Pearson, 2006.